

Multiferroic properties in nanostructured multilayered magnetic semiconductor $\text{Bi}_{0.9}\text{La}_{0.1}\text{Fe}_{0.9}\text{Co}_{0.1}\text{O}_3\text{-BiFeO}_3$ thin films

V. Annapu Reddy^{1,2,3}, Navneet Dabra^{4,5*}, K. K. Ashish¹, Jasbir S. Hundal⁵, N. P. Pathak³, R. Nath¹

¹*Ferroelectric Materials and Devices Research Laboratory, Department of Physics, Indian Institute of Technology Roorkee, Uttarakhand 247667, India*

²*Functional Ceramics Research Group, Korea Institute of Materials Science (KIMS), Changwon, Gyeongnam 641831, Korea*

³*Radio Frequency Integrated Circuits Research Laboratory, Electronics and Communication Engineering, Indian Institute of Technology Roorkee, Uttarakhand 247667, India*

⁴*Mata Sahib Kaur Girls College (affiliated to Punjabi University, Patiala), Talwandi Sabo 151302, Punjab, India*

⁵*Materials Science Laboratory, Department of Applied Physics, Giani Zail Singh Punjab Technical University Campus, Bathinda 151001, Punjab, India*

*Corresponding author. E-mail: navneetdabra@gmail.com

Received: 11 January 2015, Revised: 13 April 2015 and Accepted: 17 April 2015

ABSTRACT

Multilayers with nanostructured thin films of $\text{Bi}_{0.9}\text{La}_{0.1}\text{Fe}_{0.9}\text{Co}_{0.1}\text{O}_3\text{-BiFeO}_3$ (BLFCO-BFO) were grown on $\text{Zn}_{0.91}\text{Mn}_{0.09}\text{O}$ (ZMO) buffered Si (100) substrate by chemical solution deposition. Structural analysis indicates that rhombohedral crystal structure of BFO, changes to orthorhombic for BLFCO film. Increased ferroelectric saturation and reduced leakage current were obtained for bi-layered and four-layered thin films and are compared with those of BFO and BLFCO thin films. Improvement in ferroelectric properties, as well as induced ferromagnetism was enhanced for four-layered thin films than two-layered thin films. The interface coupling and interaction between the thin layers has led to the resultant improvements. Highly enhanced ferroelectric fatigue properties are observed in these multilayer films up to 10^8 switching cycles. Copyright © 2015 VBRI Press.

Keywords: Multilayers; nanostructures; multiferroic; magnetic semiconductor thin films; spin coater.

Introduction

Complex oxides span a wide range of crystalline structures and hosts to an incredible variety of physical phenomena. A few of the functionalities are magnetic exchange bias, diode like behaviour, ferro-, pyro- and piezoelectricity which are just offered by this class of materials. The potential for applications of the most exotic properties like magnetoelectric coupling and giant magnetoresistance is still waiting to be fully exploited. Recent progress in thin film oxide deposition techniques has enabled the fabrication of structural quality nanostructures composed of complex transition metal oxides, opening the way to unfold the physical phenomena that arise at the interface between these multifunctional materials.

The extent of complex oxides covers a wide range periodic arrangement of atoms/ molecules/ ions composing a crystal, and plays a magnificent role leading to a variety of physical phenomena. A few functionalities that were put forwarded by complex oxides are magnetic exchange bias, diode like behaviour, ferro-, pyro-, and piezoelectricity. Exotic materials are typically non ferrous and many exhibit properties like magnetoelectric coupling and giant

magnetoresistance that make them favorable for specific advanced industrial applications.

A number of novel physical phenomena at complex oxide interfaces have more recently been discovered. The ferroelectric switching change an accumulation of spin-polarized electrons at the interface of ferromagnetic/ferroelectric that affects the interface magnetization [1], an unconventional type of ferroelectricity in ferroelectric/ paraelectric structures [2], a superconducting electron gas between two dielectrics [3, 4] and enhanced critical temperatures in superconductor nanostructures that are only a few examples where interface effects play a crucial role. However, the nanostructures with multiferroic and magnetic semiconductor oxides where lateral epitaxy can develop, theoretical thermodynamic analysis [5] predicts the strong elastic interactions between the two phases promoting a rich ferroelectric and magnetic properties and hence strong magnetoelectric coupling.

A strong elastic interaction due to the lattice mismatches promoting rich ferroelectric and magnetic properties and hence strong magnetoelectric coupling. Proximity effects between multiferroics and magnetic semiconductors are exchange-bias-based devices, ferroelectric and magnetic tunnel junctions that are only a

few examples of the active fields where interface effects play a key role. The central theme is matching materials across the interface with disparate physical, chemical, electronic or magnetic structure to harness interfacial reconstructions in the strongly coupled charge, spin, orbital, and lattice degrees of freedom.

Heterostructures in the form of composites/ multilayers have shown improved ferroelectric, ferromagnetic, multiferroic properties and heterostructures with different complex oxides, which explore the control of the magnetic spin state by electric field or conversely have much attracted in the field of magnetic field sensor, magnetoelectric storage and spintronics devices [6-10]. The spin, charge, lattice and orbital degree of freedoms across the interfaces of heterostructure can have enabled the possibility to manipulate and control novel functionalities. For example, (i) the interfacial strain due to the lattice mismatch can lead to modulation of ferromagnetic anisotropy and enhancement in electrical properties, and (ii) the ferroelectric switching change an accumulation of spin-polarized electrons at the interface of ferromagnetic/ferroelectric (FM/FE) that affects the interface magnetization, as was predicted for the Fe/BaTiO₃ [11], Co₂MnSi/BaTiO₃ [12] and Fe₃O₄/BaTiO₃ [13] heterostructures.

Multiferroic BiFeO₃ (BFO) is a promising material due to the coexisted and coupled anti-ferromagnetic and ferroelectric orders at room temperature that leads to spin-based devices with ultralow power consumption and novel microwave components [14, 15]. The magnetization and polarization in single crystal BFO are quite small which prohibit its direct use in practical applications. Recent studies on BFO have confirmed the existence of large magnetization and ferroelectric polarization in strained thin films. It has been reported very recently that the heterostructure of BFO such as La_{0.7}Sr_{0.3}MnO₃ (LSMO)/BFO, Fe₂O₄/BFO, CoFe/BFO, Co/BFO, Ni/BFO and BiTiO₃/BFO show improvement in the electric and magnetic properties, as well as a large magnetoelectric coupling, due to the interface coupling interaction between the thin layers [16-18]. However, the interface coupling interaction between the thin layers is still a subject of debate.

The incorporation of buffer layer between substrate and thin film can also play an important role in improving the electric and magnetic properties of the thin films by tailoring orientation of the film. Indeed, a variety of buffer layers have been used for growth of BFO and improving the leakage current and then the multiferroic properties [19-21]. The field of ferromagnetism in dilute magnetic semiconductors (DMSs) has developed into an important branch of materials science. Metal oxides wide band-gap (ZnO and Ti₂O) are the best candidates for DMS. Among the DMSs materials, Zn_{0.9}Mn_{0.1}O (ZMO) has generated much interest because of their ferromagnetic and piezoelectric behaviors at room temperature, together with a wide spectral transparency [22]. Therefore, it could be interest to investigate the feasibility of using ZMO as a buffer layer for growth of BFO and BLFCO thin films. In view of this, the multilayer heterostructure consisting of BFO, BLFCO and ZMO thin layers have been deposited by spin coating technique. The ferroelectric and magnetic

properties of multilayer heterostructure have been studied, and these results are compared with bi-layered BFO/ZMO and BLFCO/ZMO structures.

Experimental

The thin films namely BFO/ZMO (ZBF), BLFCO/ZMO (ZBLFC) and bi-layer BLFCO/BFO/ZMO (ZBF-BLFC2) and four layered BLFCO/BFO/BLFCO/BFO/ZMO (ZBF-BLFC4) were deposited on boron doped *p*-type Si (100) (electrical resistivity ~0.01 Ω-cm) using a spin-coated technique. The Zn_{0.9}Mn_{0.1}O (ZMO) thin film was directly deposited on Si substrate using a spin-coating method. The spin rate was set at 2000 rpm for 45 s to ensure uniform distribution of the precursor solution and then the wet films were dried at 575 K for 6 min. This process was repeated six times to obtain about 180 nm thin ZMO films, which were annealed at 675 K for 30 min. Then the stoichiometric BFO and BLFCO solutions (Thomas Baker Pvt. Ltd. India) of 0.01M were spin-coated on ZMO/Si structures. The details of the spin coated BFO thin films are reported in our earlier paper [23]. Pyrolysis of each layer was conducted on a hotplate at 675 K for 10 min. The as-deposited thin films were annealed at 1100 K for 2 hrs.

The crystal structure was investigated using an X-ray diffractometer (XRD) (Advanced Bruker D8 diffractometer). The XRD data were analyzed using the *Crystal Sleuth* XRD analytical software. The surface morphology and thickness were analyzed using an atomic force microscopy (AFM, NT-MDT: Model Integra) and a field emission scanning electron microscopy (FE-SEM, Quanta 200 FEG & FEI Netherlands) respectively. The data was analyzed using NOVA image analysis software. The leakage current of all the samples was measured using a programmable Keithley-617 electrometer. The ferroelectric hysteresis (*P-E*) loops and ferroelectric measurements were performed using a modified Sawyer-Tower circuit at a frequency of 500 Hz at room temperature. The *P-E* loops were recorded with a storage oscilloscope connected to a computer with standard software (SP107E, Germany). The magnetic hysteresis (*M-H*) loops were measured by a superconducting quantum interference device, SQUID magnetometer (MPMS, XL: Quantum Design).

Results and discussion

XRD analysis

Fig. 1 show the typical X-ray diffraction patterns of ZMO, BFO, ZBF, ZBLFC, ZBF-BLFC2 and ZBF-BLFC4 thin film heterostructures. **Fig. 1(a)** shows that the buffer ZMO layer is deposited on Si substrate and is free of impurities. The ZBF films exhibit a polycrystalline perovskite structure with rhombohedral R3c symmetry [24]. The detailed XRD pattern in the 2θ range of 31-33 is shown in the inset of **Fig. 1**. It is clear that the splitting peaks become weak and tend to be a single one, which indicates the crystal structure of BLFC is transforming into a tetragonal or orthorhombic structure with the doping of Co. A similar structure transition can also be found in other element doping BFO system [25]. A slight lattice reduction of the ZBLFC film (*a* = 0.5571 nm, *c* = 1.3538 nm) is observed in comparison

with the ZBF film ($a = 0.5567$ nm, $c = 1.3654$ nm). One possible elucidation may be due to the difference in the ionic radius of dopant, the ionic radius of Co^{3+} , Fe^{3+} , La^{3+} , and Bi^{3+} are 0.62 Å, 0.65 Å, 1.032 Å and 1.03 Å, respectively [26]. A small amount of impurity phase x-ray peak was identified as a cubic bismuth oxide indicated by asterisks in Fig. 1, which is due to an excess amount of bismuth used to compensate for bismuth loss during post annealing process.

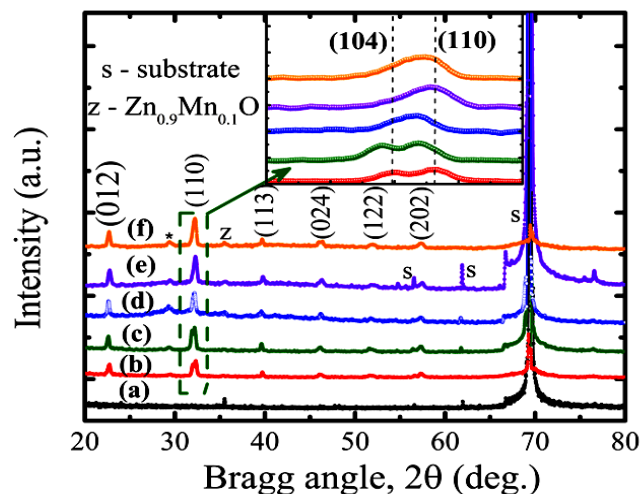


Fig. 1. XRD pattern of BFO based thin film heterostructures (a) ZMO, (b) BFO, (c) ZBF, (d) ZBLFC, (e) bi-layered ZBF-BLFC2 and (f) four-layered ZBF-BLFC4 thin film heterostructures.

On comparison with the bulk BFO ($a = 0.55923$ nm), a tensile strain have been observed in both ZBF (0.44 %) and ZBLFC (0.38 %) films. Shifting and emerging of the (110) and (104) diffraction peaks have also been observed in bi-layered ZBF-BLFC2 and four layered ZBF-BLFC4 thin films, which clearly indicates a structural transformation induced by ZBLFC layer. It should be noted that the BFO-BLFMO interface is under compressive strain (0.061 %) in contrast with a tensile strain (0.061 %) for the BLFMO-BFO interface in layered thin films. The misfit strain may impact on the multiferroic properties of the films, which is via the interface constrained effect on the films rather than from the substrate materials [27].

FE-SEM analysis

The films were crack-free, fine grained, soother surface and interface with an AFM mean surface roughness of 3 nm. A clear boundary between the two different layers indicates that the BFO layer was well deposited on the top of the ZMO buffer layer. The thickness of the films were measured from cross-section image of the films using scanning electron microscope and shown in Fig. 2 (b) and thickness of the ZMO and BFO layers are estimated to be 180 and 330 nm, respectively.

Ferroelectric properties

Fig. 3(a) shows the polarization hysteresis (P - E) loops of ZBF, ZBLFC, bi-layered ZBF-BLFC2 and four layered ZBF-BLFC4 thin films measured at room temperature. The remanent polarization (P_r) has increased about 22 % in ZBLFC films ($P_r = 9.9 \mu\text{C}/\text{cm}^2$) as compared to ZBF films

($P_r = 8.1 \mu\text{C}/\text{cm}^2$). It is well known that the oxygen vacancies, the valence fluctuation of Fe ions as well as the impurity phase could effect on polarization in ferroelectric films. The oxygen vacancies with sufficient hopping mobility and the impurity phase could assemble into an extended structure in the vicinity of domain walls, so as to impede the nucleation of new domains and cause strong domain pinning giving rise to the decrease in the polarization [8, 9, 24, 25, 32, 33].

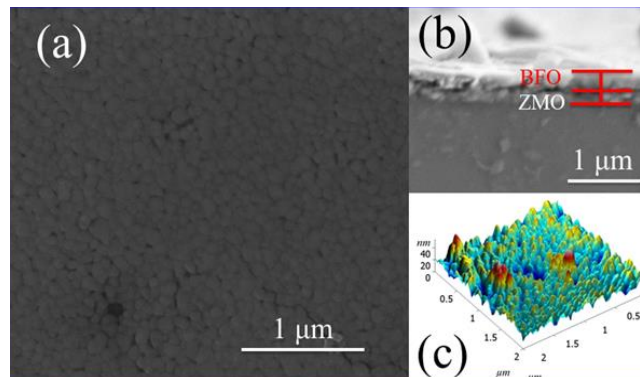


Fig. 2. (a) FE-SEM surface, (b) Cross-sectional and (c) corresponding 3D AFM images of ZBF thin film.

The oxygen vacancies and impurity phase rather than Fe^{2+} ions have been approved to be the main cause of higher leakage current in BFO films. The co-doping of La and Co in BFO can suppress the formation of oxygen vacancies, which is always reflected by reduced leakage current. Leakage current measurements presented in Fig. 3 (b) confirm that, indeed, at a field of 150 kVcm^{-1} the current density (J) for the BFO layer is already as high as $J = 10^{-2} \text{ Acm}^{-2}$. This high leakage current could also be revealed the presence of impurity phase and oxygen vacancies. In the case of the BLFCO film, the leakage current density is reduced by one order of magnitude compared with BFO alone, down to 10^{-3} Acm^{-2} at 150 kV cm^{-1} , in good agreement with the reported values for doped BFO thin films [9, 24-27]. It indicates that the smaller number of oxygen vacancies lead to the lower density of space charge and hence, lower conductivity in ZBLFC films. Therefore, for ZBLFC films, we found improvement in the ferroelectric properties.

The remanent polarization, P_r value was further proved in bi-layered ZBF-BLFC2 ($12.9 \mu\text{C}/\text{cm}^2$) films and is about 30 % larger than ZBLFC films. The improvement in the remanent polarization of the bi-layered thin films can be attributed to the interface coupling interactions between the thin layers, and/or thin BLFCO layer. But the BLFCO thin film with same thickness shows a small P_r value than bi-layered thin film, and hence it can be ruled out as the origin of the enhanced P_r value. The interface coupling interactions between the thin layers may therefore cause the resultant polarization. This is also confirmed in four layered ZBF-BLFC4 thin films. On comparison with the bi-layered films, the P_r value was increased about 27 % in four layered thin films.

It has been reported that the interface coupling interactions can be induced by the effect of interfacial strain, charge transfer, and electrostatic coupling [8, 24,

25]. Such interface coupling interactions on ferroelectric behavior is consistent with those observations in other layered structures [24-27]. Theoretical thermodynamic analysis predicts that a strong polarization-strain coupling makes them highly sensitive to the interfacial strain generated at the interface between two phases with different lattice parameters promotes an improvement in ferroelectric properties [27, 28]. This is similar to the results shown in Fig. 3(a). From XRD measurements, it can be inferred that the strain acting on layered thin films is actually +0.44 % and -0.061 % for ZMO-BFO and BFO-BLFCO interfaces, respectively. Therefore, the interface polarization-strain coupling may result in an improvement in the ferroelectric properties of the layered BFO structures.

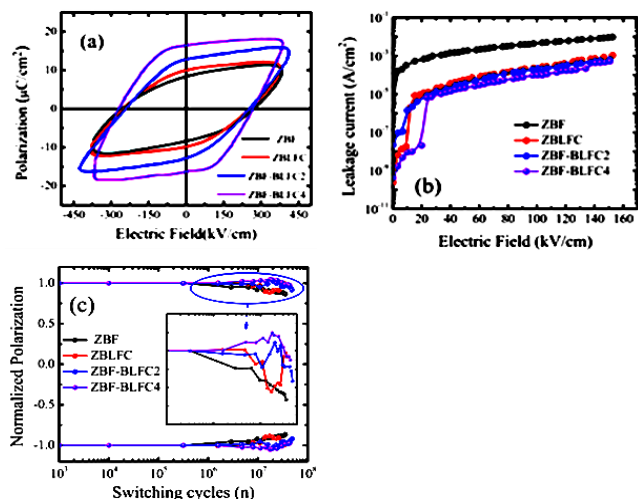


Fig. 3. (a) Polarization hysteresis, (b) leakage current characteristics and (c) fatigue studies of BFO based thin films.

The endurance to ferroelectric fatigue was examined for all thin films as shown in Fig. 3(c). The BFO films showed a reduction of 15% after 10^8 switching cycles. This poor resistance to fatigue of our BFO films is however, still superior to the 50% degradation after 10^8 switching cycles observed in BFO films prepared by spray pyrolysis method [8, 21, 24]. As expected, BLFCO thin films do not show any significant polarization degradation up to 10^8 switching cycles. The ferroelectric fatigue in perovskite oxides is essentially related to the diffusion and relocation of the oxygen vacancies, and electronic-charge trapping at the domain wall during the electric switching [24-28]. The reduction in the movable charge density is the direct reason for the improved fatigue behavior in ZBLFC samples. In addition to good ferroelectric properties, layered ZBF-BLFC2 and ZBF-BLFC4 thin films also demonstrated an excellent fatigue endurance, with less than 7% polarization reduction upon cycling the ferroelectric polarization up to 10^8 switching cycles, which is much better than the BFO films reported earlier [21], clearly demonstrating the superior insulating properties of multilayered structures.

Magnetic properties

The magnetic hysteresis ($M-H$) loops of the thin films were measured at low temperature (5K) and room temperature (300 K) by SQUID magnetometer as shown in Fig. 4. The ZBF film shows a weak ferromagnetic behavior at room

temperature. The saturation magnetization (M_s) and coercive magnetic field (H_c) are $4.5 \text{ emu}\cdot\text{cm}^{-3}$ and 91 Oe at 300 K respectively, which is in agreement with that reported value and is consistent with the fact that the thin film usually strained and increases the Fe-O-Fe bond angle in BFO thin films. Fig. 4(b) shows the $M-H$ loops of ZBLFC film. It is clear that ZBLFC film exhibits a large saturation magnetization with clear hysteresis loop, and the magnetization is evidently larger than that of ZBF. A structural transformation from a rhombohedral to a monoclinic type structure has been observed in BLFCO sample, which can lead to a modification of the spin cycloidal structure [30]. The spiral arrangement of the magnetic spins having a wavelength of 62 nm suppresses magnetization in BFO. As reported previously, the difference in magnetic moment of Co^{2+} and Fe^{3+} interrupts the spiral spin structure that result a local ferri-magnetic ordering in Co doped BFO film [30]. In addition, a small amount of secondary phase bismuth oxide observed in the films is a non-magnetic material, hence gives no contribution to magnetic properties. It may be the possible reasons that BLFCO shows a larger saturation magnetization than BFO. The coercive field ($H_c = 4.3 \text{ kOe}$ at 5K) is much higher than what has been observed in doped BFO films [9, 24-31].

The saturation magnetization, $M_s (=16.8 \text{ emu}\cdot\text{cm}^{-3}$ at 300 K) observed in bi-layered ZBF-BLFC2 film and is about four fold larger than ZBF film. The interface coupling interactions between the thin layers, and/or thin ferromagnetic layer might result improvement in magnetic behavior of layered structure. A large magnetization ($M_s = 23.8 \text{ emu}\cdot\text{cm}^{-3}$ at 300 K) was observed in the ZBLFC sample, as discussed above, and therefore the improvement in magnetic properties in layered ZBF-BLFC2 structures must originate from the BLFCO layer. This hypothesis also confirmed in four layered ZBF-BLFC4 structure. As compared to ZBF-BLFC2 structure, improve magnetization ($M_s = 21.7 \text{ emu}\cdot\text{cm}^{-3}$ at 300 K) has been observed in four-layered ZBF-BLFC4 structure. However, the contribution of interface coupling interactions between the thin layers to magnetization cannot be completely ignored especially in layered structures [19, 28, 30, 33-38].

The interface coupling interactions directly influence coupling between the BFO and the BLFCO upon freezing at low temperatures and produced the pinned, uncompensated spins that induces exchange bias, $H_{EB} = -(H_1 + H_2)/2$, where H_1 and H_2 are defined as the left and right coercive field at the loop centered in the magnetization axis (Fig. 4). Having established this, the magnetic hysteresis loops were measured at low temperature (5 K) as shown in Fig. 4. The buffer ZMO layer shows ferromagnetic behavior at low temperature ($>45 \text{ K}$), hence gives contribution to magnetic properties. The large magnetization and the large coercive field at low temperature come from the phase of ZMO and the local clustering of spins and not the other magnetic impurities.

The measured H_{EB} value for ZBF, ZBLFC, ZBF-BLFC2 and ZBF-BLFC4 films were 4, 18, 142 and -136 Oe respectively are tabulated in Table 1. The values of M_s , H_c , at 5K and 30K, and H_{EB} for ZBF, ZBLFC, ZBF-BLFC2 and ZBF-BLFC4 nanostructured films have been tabulated in Table 1. A similar phenomenon has been observed in

earlier studies on LSMO/BFO and $\text{Fe}_2\text{O}_3/\text{BFO}$ heterostructures [11–13]. These results suggest interface coupling interaction between the ZMO and BFO and BLFCO thin layers may also contribute to improve magnetic properties.

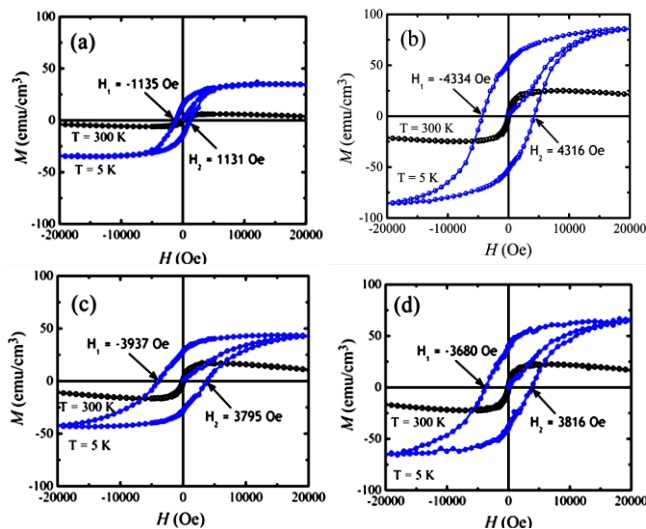


Fig. 4. M-H loops for (a) ZBF, (b) ZBLFC, (c) bi-layered ZBF-BLFC2 and (d) four-layered ZBF-BLFC4 thin films, measured with magnetic fields applied parallel to the plane of the films at 5 K and 300 K.

Table 1. Various magnetic parameters of nanostructured multilayered magnetic semiconductor thin films.

Sample Name	5 K		300 K		H_{EB} (Oe) at 5 K
	M_s (emu-cm ⁻³)	H_c (Oe)	M_s (emu-cm ⁻³)	H_c (Oe)	
ZBF	35.0	1133	4.5	91	4
ZBLFC	85.7	4325	23.8	111	18
ZBF-BLFC2	43.1	3866	16.8	188	142
ZBF-BLFC4	65.1	3748	21.7	132	-136

Conclusion

Layered magnetic semiconductor thin films of ZMO, BFO and BLFCO have been fabricated by the spin-coating method and characterized. The leakage current has significantly reduced in the four-layered thin films. The ferromagnetic and magnetic properties have greatly improved compared to BFO films. The high stability of remanent polarization was observed in the films. The interface coupling and interaction between the constrained layers improves the magnetic and ferroelectric properties.

Acknowledgements

The author V. Annapu Reddy acknowledges the financial support provided by Ministry of Human Resources and Development (MHRD) and Council of Scientific and Industrial Research (CSIR), Government of India. Authors (Dr. Dabra and Dr. Hundal), acknowledge the Punjab Technical University, Kapurthala (Punjab) for providing research facilities.

Reference

- Stognij, A.I.; Novitskii, N.N.; Sharko, S.A.; Bespalov, A.V.; Golikova, O.L.; Sazanovich, A.; Dyakonov, V.; Szymczak, H.; Ketsko, V.A.; *Inorg. Mat.* **2014**, *50*, 280.
DOI: [10.1134/S0020168514030133](https://doi.org/10.1134/S0020168514030133)
- Bousquet, E.; Dawber, M.; Stucki, N.; Lichtensteiger, C.; Hermet, P.; *Nature*, **2008**, *452*, 732.

- DOI: [10.1038/nature06817](https://doi.org/10.1038/nature06817)
- Ohtomo, A.; and Hwang, H.Y.; *Nature*, **2004**, *427*, 423.
DOI: [10.1038/nature02308](https://doi.org/10.1038/nature02308)
- Reyren, N.; Thiel, S.; Cavaglia, A. D.; Kourkoutis, L. F.; Hammer, G.; *Science*, **2007**, *317*, 1196.
DOI: [10.1126/science.1146006](https://doi.org/10.1126/science.1146006)
- Sharma, P.; Gupta, A.; Rao, K. V.; Owens, F. J.; Sharma, R.; Ahuja, R.; Osorio Guillen, J. M.; Johansson, B.; Gehring, G. A.; *Nature Materials*, **2003**, *2*, 673.
DOI: [10.1038/nmat984](https://doi.org/10.1038/nmat984)
- Dabra, N.; Hundal, J. S.; Jeong, D. Y.; Kaur, B.; Nautiyal, A.; Reddy, V. A.; Nath, R.; *Materials Focus*, **2013**, *2*, 454.
DOI: [10.1166/mat.2013.1122](https://doi.org/10.1166/mat.2013.1122)
- Dabra, N.; Hundal, J. S.; Sekhar, K. C.; Nautiyal, A.; Nath, R.; *IEEE Trans. On Ultra., Ferro., and Freq. Cont.*, **2009**, *56*, 1627.
DOI: [10.1109/TUFFC.2009.1227](https://doi.org/10.1109/TUFFC.2009.1227)
- Reddy, V. A.; Dabra, N.; Hundal, J. S.; Pathak, N. P.; Nath, R.; *Science of Advanced Materials*, **2014**, *6*, 235.
DOI: [10.1166/sam.2014.1707](https://doi.org/10.1166/sam.2014.1707)
- Reddy, V. A.; Sekhar, K. C.; Dabra, N.; Nautiyal, A.; Hundal, J. S.; Pathak, N. P.; Nath, R.; *d Materials Science Volume 2011*, **2011**, Article ID 142968.
DOI: [10.5402/2011/142968](https://doi.org/10.5402/2011/142968)
- Kumar, A.; Yadav, K. L.; *Physica B: Condensed Matter*, **2011**, *406*, 1763.
DOI: [10.1016/j.physb.2011.02.023](https://doi.org/10.1016/j.physb.2011.02.023)
- Valencia, S.; Crassous, A.; Bocher, L.; Garcia, V.; Moya, X.; Cherifi, R. O.; Deranlot, C.; Bouzouane, K.; Fusil, S.; Zobel, A.; Gloter, A.; Mathur, N. D.; Gaupp, A.; Abrudan, R.; Radu, F.; Barthélémy, A.; *Nature Materials*, **2011**, *10*, 753.
DOI: [10.1038/nmat3098](https://doi.org/10.1038/nmat3098)
- Chen, L. Y.; Chen, C. L.; Jin, K. X.; Du, X. J.; *EPL*, **2012**, *99*, 57008.
DOI: [10.1209/0295-5075/99/57008](https://doi.org/10.1209/0295-5075/99/57008)
- Qu, T. L.; Zhao, Y. G.; Yu, P.; Zhao, H. C.; Zhang, S.; Yang, L. F.; *Appl. Phys. Lett.* **2012**, *100*, 242410.
DOI: [10.1063/1.4729408](https://doi.org/10.1063/1.4729408)
- Catalan G.; Scott, J. F.; *Adv. Mater.*, **2009**, *21*, 1.
DOI: [10.1002/adma.200802849](https://doi.org/10.1002/adma.200802849)
- Bibes, M.; Barthélémy, A.; *Nature Mat.* **2008**, *7*, 425.
DOI: [10.1038/nmat2189](https://doi.org/10.1038/nmat2189)
- Xu, Q.; Wen, Z.; Gao, J.; Wu, D.; Tang, S.; Xu, M.; *Physica B*, **2011**, *406*, 2025.
DOI: [10.1016/j.physb.2011.03.011](https://doi.org/10.1016/j.physb.2011.03.011)
- Singh, H.; Kumar, A.; Yadav, K. L.; *Mat. Sci. Eng. B*, **2011**, *176*, 540.
DOI: [10.1016/j.mseb.2011.01.010](https://doi.org/10.1016/j.mseb.2011.01.010)
- Reddy, V. A.; Dabra, N.; Hundal, J. S.; Pathak, N. P.; Nath, R.; *Science of Advanced Materials*, **2014**, *6*, 1043.
DOI: [10.1166/sam.2014.1865](https://doi.org/10.1166/sam.2014.1865)
- Bertinshaw, J.; Cortie, D. L.; Cheng, Z. X.; Avdeev, M.; Studer, A. J.; Klose, F.; Ulrich, C.; Wang, X. L.; *Phys. Rev. B*, **2014**, *89*, 144422.
DOI: [10.1103/PhysRevB.89.144422](https://doi.org/10.1103/PhysRevB.89.144422)
- Wu, J.; Wang, J.; *J. Appl. Phys.* **2009**, *106*, 054115.
DOI: [10.1063/1.3213335](https://doi.org/10.1063/1.3213335)
- Wu, J.; Wang, J.; *J. Appl. Phys.* **2010**, *108*, 034102.
DOI: [10.1063/1.3460108](https://doi.org/10.1063/1.3460108)
- Cheng, X. M.; Chien, C. L.; *J. Appl. Phys.*, **2003**, *93* (No. 10, Parts 2 & 3), 7876.
DOI: [10.1063/1.1556125](https://doi.org/10.1063/1.1556125)
- Reddy, V. A.; Pathak, N. P.; Nath, R.; *Solid State Commun.* **2013**, *171*, 40.
DOI: [10.1016/j.ssc.2013.07.032](https://doi.org/10.1016/j.ssc.2013.07.032)
- Reddy, V. A.; Dabra, N.; Hundal, J. S.; Pathak, N. P.; Nath, R.; *Sci. Adv. Mat.* **2014**, *6*, 1228.
DOI: [10.1166/sam.2014.1922](https://doi.org/10.1166/sam.2014.1922)
- Yuan, G. L.; Ora, S. W.; Liu, J. M.; Liu, Z. G.; *Appl. Phys. Lett.* **2006**, *89*, 052905.
DOI: [10.1063/1.2266992](https://doi.org/10.1063/1.2266992)
- Shannon, R. D.; *Acta Crystallogr.* A32:751, 1974 (From Handbook Of Chemistry And Physics, 74th Edition, CRC Press, Boca Raton, FL, 1974).
- Schlom, D. G.; Chen, L. Q.; Eom, C. B.; Rabe, K. M.; Streiffer, S. K.; Annu, J. M. T.; *Rev. Mater. Res.*, **2007**, *37*, 589.
- Kukhar, V. G.; Pertsev, N. A.; Kholkin, A. I.; *Nanotechnology*, **2010**, *21*, 265701

- DOI: [10.1088/0957-4484/21/26/265701](https://doi.org/10.1088/0957-4484/21/26/265701)
29. Yang, K. G.; Zhang, Y. L.; Yang, S. H.; Wang, B.; *J. Appl. Phys.* **2010**, *107*, 124109.
DOI: [10.1063/1.3437232](https://doi.org/10.1063/1.3437232)
30. Rahmedov, D.; Wang, D.; Íñiguez, J.; and Bellaiche, L.; *Phys. Rev. Lett.*, **2012**, *109*, 037207.
DOI: [10.1103/PhysRevLett.109.037207](https://doi.org/10.1103/PhysRevLett.109.037207)
31. Rani, R.; Juneja, J. K.; Singh, S.; Raina, K. K.; Prakash, C; *Adv. Mat. Lett.* **2014**, *5*, 229.
DOI: [10.5185/amlett.2013.fdm.63](https://doi.org/10.5185/amlett.2013.fdm.63)
32. Annapu, Reddy V.; Varma, G. D.; Nath, R.; *AIP Advances*, 2011, *1*, 042140.
DOI: [10.1063/1.3662093](https://doi.org/10.1063/1.3662093)
33. Kaushik C.; Kajari D.; Babusona S.; Sirshendu G.; De S. K.; Godhuli S.; Lahtinen J.; *Appl. Phys. Lett.* **2012**, *101*, 042401.
DOI: [10.1063/1.4738992](https://doi.org/10.1063/1.4738992)
34. Rai, R.; Coondoo, I.; Valente, M. A.; Kholkin, A.L.; *Adv. Mat. Lett.* **2013**, *4*, 354.
DOI: [10.5185/amlett.2012.9428](https://doi.org/10.5185/amlett.2012.9428)
35. Chandra, U.; Asokan, K.; Ganesan, V.; *Adv. Mat. Lett.* **2013**, *4*, 862.
DOI: [10.5185/amlett.2013.4455](https://doi.org/10.5185/amlett.2013.4455)
36. Sharma, P. K.; Dutta, R. K.; Pandey, A.C.; *Adv. Mat. Lett.* **2011**, *2* (4), 246.
DOI: [10.5185/amlett.2011.indias214](https://doi.org/10.5185/amlett.2011.indias214)
37. Suresh, P.; Srinath, S.; *Adv. Mat. Lett.* **2014**, *5*(3), 127.
DOI: [10.5185/amlett.2013.fdm.34](https://doi.org/10.5185/amlett.2013.fdm.34)
38. Gaikwad, V. M.; Acharya, S. A.; *Adv. Mat. Lett.* **2014**, *5*(3), 157.
DOI: [10.5185/amlett.2013.fdm.82](https://doi.org/10.5185/amlett.2013.fdm.82)

Advanced Materials Letters

Copyright © VBRI Press AB, Sweden

www.vbripress.com

Publish your article in this journal

Advanced Materials Letters is an official international journal of International Association of Advanced Materials (IAAM, www.iaamonline.org) published by VBRI Press AB, Sweden monthly. The journal is intended to provide top-quality peer-review articles in the fascinating field of materials science and technology particularly in the area of structure, synthesis and processing, characterisation, advanced-state properties, and application of materials. All published articles are indexed in various databases and are available download for free. The manuscript management system is completely electronic and has fast and fair peer-review process. The journal includes review article, research article, notes, letter to editor and short communications.

